

Glasgow Preprint GUTPA 95-9-2

Liverpool Preprint LTH 359

hep-lat/9509083

Masses and decay constants of the light mesons in the quenched approximation using the tadpole-improved SW-clover action. *

UKQCD Collaboration

C. Michael

DAMTP, University of Liverpool, Liverpool, L69 3BX, U.K.

H. Shanahan

Department of Physics and Astronomy, University of Glasgow, Glasgow, G12 8QQ, Scotland, U.K.

Abstract

We present results for the masses and decay constants of the light mesons in quenched QCD using the standard gluon action and a tadpole-improved SW-clover fermionic action to reduce discretisation errors. The calculation has been carried out at fixed volume and three lattice spacings corresponding to $\beta = 5.7, 6.0$ and 6.2 . We make comparisons with the conventional SW-clover scheme. We use our results to extract continuum limits and to quantify the size of discretisation errors at smaller β -values.

*Presented at the XIIIth International Symposium on Lattice Field Theory, Melbourne, Australia, July 11-15, 1995.

I. INTRODUCTION

To extract reliable continuum results from lattice studies, it is essential to explore a range of β -values. It is also valuable to employ a fermionic discretisation which has minimal discretisation errors. Here we investigate the tadpole-improved clover-SW action and we present preliminary results for the quenched spectrum at three lattice spacings. We compare our light hadron results at $\beta = 6.2$ with the conventional SW-clover approach and find no statistically significant evidence of further improvement at that β -value.

We use non-local sources to allow a more accurate extraction of ground state masses and couplings. Combining our results at all three β -values, we can extract the continuum limit and assess the size of discretisation effects. We find that dimensionless ratios of observables have small discretisation corrections. We highlight the uncertainties remaining in extracting continuum decay constants because of the reliance on perturbative matching coefficients.

II. THE SW CLOVER ACTION

The SW fermion action is written in the form

$$S_F^C = S_F^W(\kappa) - \kappa c S_{\text{clover}} \quad (1)$$

with hopping parameter κ . The quark fields q and \bar{q} which appear in any observable must also be transformed (rotated). For an on-shell observable bilinear in the quark fields, the equation of motion can be used to express this as an improved observable given by [1,2]

$$O_\Gamma^{\text{imp}} = (1 + am_q(1 - z))\bar{q}(\Gamma + z\Gamma^\otimes)q \quad (2)$$

where $0 \leq z \leq 1$. The size of the clover term in the action is determined by the coefficient c . At tree-level, c is equal to one. As demonstrated by Heatlie *et al.* [1], the terms of order a are removed for this choice of c .

A mean field estimate of this coefficient was suggested by Lepage and Mackenzie [3]. In this approach, the poor agreement of lattice perturbation theory with Monte Carlo simula-

tions of short-distance observables is explained by the presence of non-physical “tadpole” diagrams. One expects the power expansion for the gauge link

$$U_\mu(x) = 1 + i a g A_\mu(x) + \mathcal{O}(a^2 g^2) , \quad (3)$$

to be valid for sufficiently small a . However, tadpole diagrams introduce ultraviolet divergences which can partly cancel the factors of a^2 . A solution to this is to rescale the gauge link by a factor u_0 , such that $U_\mu(x) \rightarrow \tilde{U}_\mu(x) = U_\mu(x)/u_0$. The factor u_0 is chosen so that a Monte Carlo calculation of a short distance observable using the rescaled gauge field agrees with the perturbative calculation. An appropriate choice is

$$u_0 = \left\langle \frac{1}{3} \text{Tr} U_{\text{plaq}} \right\rangle^{1/4} . \quad (4)$$

Inserting this factor into the SW action changes the hopping parameter to $\tilde{\kappa} = \kappa u_0$ and the clover coefficient c from 1 to u_0^{-3} . A perturbative evaluation of c by Naik [4] gives a numerically similar value which is some support for the assumption of dominance of the tadpole diagrams.

A. Computational Details

Gauge configurations were calculated at $\beta = 5.7, 6.0$ and 6.2 , using spatial volumes that are approximately the same. At each lattice spacing, propagators at 2 quark masses, straddling the strange quark mass, were calculated for each configuration — see table 1. Hadronic correlations were evaluated for each combination of such quarks, yielding three mesonic masses. Hence the extrapolation to the chiral limit could be explored using three hadronic masses. The configuration and propagators at $\beta = 6.0$ and 6.2 were calculated on a 320 node Cray T3D. The gauge configurations and propagators at $\beta = 5.7$ were calculated respectively on a 16 and 64 node i860 Meiko Computing Surface. For the transformation in eq. 2, we take $z = 0$ which corresponds to no rotation in the propagators.

The propagators were calculated using both non-local and local sources so that ground state and excited state contributions to correlators could be separated effectively. Local

sinks were employed. At $\beta = 5.7$, Jacobi smeared sources [5] were used, and correlations were measured with three combinations (neither, one, both) of nonlocal and local quark propagators in a meson. At $\beta = 6.0$, local and “fuzzed” sources were used [6]. A fuzzed source can be written in the form

$$S_{\text{fuzzed}}(x) = \sum_{i=1}^3 \sum_{y_i=\pm r} F(y) \delta(x - y_i) , \quad (5)$$

where $F(y)$ is an SU(3) matrix representing the average of the fuzzed paths of gauge links from the origin to (y) (see fig. 1 for a schematic description). Fuzzing is less computer expensive than Jacobi smearing, as the only numerical work involves the averaging of the gauge links. It is gauge invariant and avoids time spent in gauge fixing. We use the fuzzing prescription with 5 iterations as in ref. [6] and we choose $r = 6a$ at $\beta = 6.0$. An example of the advantage of fuzzing at the source is shown in fig. 2 where an efficient extraction of the ground state vector meson is seen.

III. FITTING

We focus on the pseudoscalar and vector mesons. In order to evaluate accurately the central value and statistical errors, we fit to as many channels of data as possible. Furthermore, to isolate the ground state for a wide range of time slices, we use a two-exponential fit.

The two-point correlations can be expressed as a sum over transfer matrix eigenstates

$$\sum_{\vec{x}} \langle 0 | O_2(\vec{x}, t) O_1^\dagger(0) | 0 \rangle = \sum_i \frac{c_2^i c_1^{i*}}{m_i} \cosh m_i(t - N_t/2) . \quad (6)$$

Here $c^i = \langle 0 | O | H^i \rangle$ where $O_{1,2}$ are operators that have overlap with the ground and excited mesonic states $|H^0\rangle$ and $|H^1\rangle$. These operators can be local or nonlocal, or have different gamma matrix structures. For both mesons, we fit simultaneously to all the available local and non-local source correlations of two-point functions.

In the case of the pseudoscalar, we note that the fields $P(x) = \bar{q}(x)\gamma^5 q(x)$ and $A(x) = \bar{q}(x)\gamma^0\gamma^5 q(x)$ will create/annihilate the pseudoscalar, hence a simultaneous fit is performed

to two-point functions with the four combinations PP, AP, PA, AA. These contributions can be described in a factorising fit by the amplitudes $\langle 0|A|PS\rangle$ and $\langle 0|P|PS\rangle$, where $|PS\rangle$ is the pseudoscalar state. This provides tight constraints on the fit.

We define the lattice decay constant for a pseudoscalar meson, \hat{f}_{PS} as :

$$\langle 0|A_L|PS\rangle = m_{PS}\hat{f}_{PS} , \quad (7)$$

where A_L is the *local* axial current operator. The lattice \hat{f} will be related to the continuum value f by including quark field rotations, setting the scale a and including the appropriate matching coefficient Z_A . One can determine \hat{f}_{PS} directly from the factorising fit, without fitting to a ratio of channels as was used previously [7]. An example of the result of such fits is shown in fig. 3.

Likewise, simultaneous fits for the vector meson can be performed using the operators $V_1^i = \bar{q}\gamma^i q$ and $V_2^i = \bar{q}\gamma^0\gamma^i q$, and different smearing/fuzzing combinations. The lattice vector decay constant, \hat{f}_V is defined by

$$\sum_{j=1}^3 \sum_{\vec{x}} \langle V_1^j(\vec{x}, t) V_1^{j\dagger}(0) \rangle \rightarrow \frac{3m_V^2}{\hat{f}_V^2} \cosh m_V(t - N_t/2) + A_V^* \cosh m_V^*(t - N_t/2) , \quad (8)$$

where V_1^j is the local vector current.

Despite the quite large statistics used in this calculation, the large number of different types of two-point functions requires that a full correlated fit must be carried out carefully. In particular, we employ the methods described by Michael and McKerrell [8] for the inversion of the correlation matrix. At $\beta = 6.0$ and 6.2 , we model the correlation matrix with two exponents using the 5-diagonal approximation of ref. [8]. At $\beta = 5.7$, we average all but 20 of the largest eigenvalues of the correlation matrix. We fit to the largest range of t consistent with an acceptable χ^2 . The errors quoted in this preliminary report are statistical only.

IV. RESULTS: MASSES

A. Chiral Extrapolation

The ground state pseudoscalar and vector masses are determined by the fits to two-particle correlations as described above. The issue of the rotations of the quark fields is irrelevant to mass determinations and will be discussed later. We define $\kappa_{\text{crit}}(\beta)$ by the requirement $m_{PS}^2 = 0$ for each lattice. At each lattice spacing, a linear extrapolation in the two squared pseudoscalar masses (where the quark masses are degenerate) was carried out. The results for $\tilde{\kappa}$ are given in table 2. A full fit using also the meson mass determined from the non-degenerate quark-mass case is possible, however, the fits gave statistically significant evidence for some curvature in m_{PS}^2 versus $1/\kappa$.

Without tadpole-improvement, there has been no agreement of non-perturbative lattice determinations of $\kappa_{\text{crit}}(\beta)$ with one loop perturbation theory. For Wilson-like fermion actions, it is found that the tadpole-improvement factor of u_0 makes $\tilde{\kappa}_{\text{crit}}$ closer to the tree-level value of $1/8$. For example, a determination of κ_{crit} using the $c = 1$ clover action [7] at $\beta = 6.2$ gave a result of $\kappa_{\text{crit}} = 0.14315 \pm 2$ which corresponds to $\tilde{\kappa}_{\text{crit}} = 0.12670 \pm 2$.

For the tadpole-improved action explored here, we present in table 2 the comparison of the non-perturbative results for $\tilde{\kappa}_{\text{crit}}$ with the one loop perturbative calculation. Here we have chosen to use a coupling derived from $\alpha = -\frac{3}{4\pi} \log S_{\text{plaq}}$. Although the agreement is excellent at $\beta = 6.2$, the trend as β is decreased is not. This lack of agreement of κ_{crit} between non-perturbative determinations and one-loop perturbation theory at smaller β will cause some uncertainty in normalisation when quark mass factors are included in the determination of the decay constants.

B. $m_V^2 - m_{PS}^2$

The experimental value of the difference $m_V^2 - m_{PS}^2$ remains remarkably constant, at approximately 0.55 GeV^2 , over a wide range of masses. Quenched lattice simulations of relativistic quarks have been in poor agreement with this result, and the discrepancy increases

as the quark mass is increased. In the heavy quark regime, such splitting has a leading order dependence on the chromo-magnetic coupling of the heavy quark with the gluon field. This is precisely the term which is amplified in the tadpole-improved clover action. While one cannot make a similar statement in the light quark regime, it is plausible that this modification of the clover term will also have a significant effect there.

A comparison at $\beta = 6.2$ can be made with non tadpole-improved UKQCD data [7,9], based on 60 configurations. These configurations exist as a subset of the 184 configurations available now. A comparison of the results is shown in fig. 4. Unfortunately, there is no significant statistical difference between the two actions. We will soon have results for fussed sources in the tadpole-improved mass extraction which should lead to a reduction of errors.

The behaviour at all three lattice spacings is shown in fig. 5. The scale (a_ρ^{-1}) is determined from the chirally extrapolated m_ρ . The fall-off of the splitting with respect to m_{PS}^2 is slightly faster than one would expect by comparison with the physical splittings $m_\rho^2 - m_\pi^2$ and $m_{K^*}^2 - m_K^2$. However, until this difference is examined for quark masses around that of the charm quark, the advantage of tadpole improvement in this case remains unproven.

C. Discretisation effects

The dimensionless ratio of masses is known to have discretisation errors of order αa for the SW-clover fermionic action. The tadpole-improved variant should preserve this result and is expected to improve on it by reducing the coefficient. We explore this by studying such ratios of observables against an observable proportional (to leading order) to a .

Since the Wilson gauge action has inherent discretisation errors of order a^2 , it is advantageous to use this as a reference. We present ratios of m_ρ to \sqrt{K} where K is the string tension determined by interpolating all existing data. In fig. 6, we find that the ratio is constant (within statistical errors) at $\beta = 6.0$ and $\beta = 6.2$. There is however, a significant deviation from this constant for the ratio at $\beta = 5.7$. Since this behaviour is consistent with a^2 , it could be ascribed to the discretisation errors in either (or both) of the pure-gauge or

fermionic quantities.

It is important to compare lattice results in the quenched approximation without chiral extrapolation if possible, since there are known to be anomalies in the chiral limit of a quenched theory. As suggested by Lacock and Michael [9], a dimensionless quantity can be constructed using this data without having to perform a chiral extrapolation:

$$J = m_V \frac{dm_V}{dm_{PS}^2} \quad (9)$$

where the slope and m_V are to be evaluated at the vector mass satisfying $m_V/m_{PS} = 1.8$ which corresponds to the K^* meson.

Our results are shown in fig. 7 and there is no evidence of any discretisation error since the values of J from each lattice spacing are equal within errors. Our result agrees with that from most existing quenched lattice data which are consistent [9] with a value of J of 0.37. This value is in disagreement with experimental data and, to substantiate this discrepancy, we will need a careful study of systematic errors, particularly at our largest β -value.

V. RESULTS: DECAY CONSTANTS

As can be seen from eqs. 7 and 8, the parameters \hat{f}_{PS} and $1/\hat{f}_V$ can be easily obtained from the lattice data. However, to evaluate the physical quantities f_{PS} and $1/f_V$, one has to specify a suitable normalisation for the quark propagators and a renormalisation factor for the lattice operators. For fermion actions of the kind of eq. 1, several equivalent solutions have been proposed. To estimate the size of the systematic error induced by relying on perturbative estimates of the matching factors, we present here two interpretations of the action (eq. 1) with $c = u_0^{-3}$ which result in relatively large differences.

This systematic uncertainty is due to both our ignorance on the contribution of $O(\alpha_s^2)$ terms in the perturbative expansion, and to the possible different interpretations of the tadpole improvement procedure.

Normalisation I

In this case we interpret the clover coefficient $c = u_0^{-3}$ as a consequence of the tadpole improvement, which implies a redefined hopping parameter ($\tilde{\kappa}$) and a gauge field rescaling. Because $U_\mu \rightarrow U_\mu/u_0$, the covariant derivative (or the lattice bare mass for the unrotated case $z = 0$ which we are using) which appears in eq. 2 has to be divided by u_0 . We choose, however, to adopt a slightly different normalisation, which amounts to using the renormalized quark mass,

$$am_q = \frac{1}{2} \left(\frac{1}{\tilde{\kappa}} - \frac{1}{\tilde{\kappa}_c} \right) , \quad (10)$$

instead of the bare mass since the “rotation” factor $1 + am_q$ is then relatively closer to unity and possibly better reproduced by perturbation theory. This is possible because formally the difference between the bare mass and the renormalised mass only contributes at order αa which does not effect the improvement.

The renormalisation constants to be used in this case differ from those corresponding to the SW action, and have been computed in ref. [10], and are

$$\begin{aligned} Z_A &= 1 - 0.41\alpha_s + \mathcal{O}(\alpha_s^2) , \\ Z_V &= 1 - 0.58\alpha_s + \mathcal{O}(\alpha_s^2) , \end{aligned} \quad (11)$$

where we choose to use $\alpha_s = -\frac{3}{4\pi} \log S_{\text{plaq}}$ as an appropriate improved estimate of the coupling. There is an inherent systematic error from the choice of scale for this coupling - this can only be resolved by a two-loop calculation.

Normalisation II

Let us consider the results one obtains using the action of eq. 1 with $c = u_0^{-3}$ but without attributing to such a coefficient the meaning of tadpole subtraction. Because of that both the hopping parameter and the normalisation of the propagator itself keep their original values. Moreover, since the perturbative expansion of the clover coefficient is 1, up to terms of $\mathcal{O}(\alpha)$, the renormalisation constants are the same as those calculated for $c = 1$, given in ref. [2]. In this case we used the “unrotated” operators corresponding to taking $z = 0$ in eq. 2, where m_q is now interpreted as the “bare” lattice quark mass.

In order to compare with other work, at each β , we extrapolate the lattice decay constants to the chiral limit assuming a linear behaviour with m_{PS}^2 . The dimensionless quantities f_π/\sqrt{K} and $1/f_\rho$ are shown for each normalisation in figs. 8, 9.

The results for f_π/\sqrt{K} for both normalisation schemes are consistent with having a common continuum limit which agrees with the experimental value. As β is decreased, the difference between normalisations I and II increases. This largely arises from the fact that the perturbative estimate of m_q is not in agreement with the numerical value (it is therefore due to large unknown contributions at $O(\alpha^2)$), and this causes a poor renormalisation in the case II. An insight into this problem could be achieved by calculating the “rotated” operators of eq. 2 with $z = 1$, which would permit us to eliminate the uncertainty in the renormalisation of the quark mass. Such a study is currently in progress. Ideally, however, one should measure the matching constants non-perturbatively, as outlined in refs. [11] and [12].

The $c = 1$ results [9] for f_π/\sqrt{K} at $\beta = 6.2$ are seen to lie significantly lower in fig. 8. A careful study of systematic errors is needed to explore this discrepancy further. Since we have used different rotation factors ($z = 0$ for $c = u_0^{-3}$ and $z = 1$ for $c = 1$), the effect of this difference on the discrepancy can also be determined by a study of $z = 1$ for the tadpole-improved case.

Fig. 9 shows for $1/f_\rho$ a rather similar picture of agreement between the continuum limit of the tadpole-improved schemes and experiment. In this case the $c = 1$ result is also in agreement.

VI. CONCLUSIONS

The goal of lattice investigations of QCD is to find a formalism which has small discretisation errors. This has to be studied by obtaining results for a wide range of observables for several lattice spacings. In this paper we have outlined preliminary results on the spectrum and couplings from a tadpole-improved SW clover action. We find that, within our present

statistical errors, the results at $\beta = 6.0$ and 6.2 are consistent while those at $\beta = 5.7$ show signs of discretisation effects. This is encouraging since it suggests that meaningful results can be obtained at 6.0 which corresponds to $a^{-1} > 1.8$ GeV. To push the frontier down to 5.7 , it seems plausible that an improved gauge action will also be needed since the ratio of $m(0^{++})/\sqrt{K}$ evaluated using the Wilson gauge action is known to deviate significantly at $\beta = 5.7$ so that there are significant order a^2 discretisation errors here.

We also emphasize that continuum extraction of decay constants and matrix elements is beset with ambiguity if a perturbative matching is used. This arises in part because the critical hopping parameter is not accurately given by 1 loop perturbation theory. A non-perturbative determination of these matching coefficients is essential for fully reliable continuum predictions.

REFERENCES

- [1] G. Heatlie *et al.*, Nucl.Phys. **B** 352 (1991) 266.
- [2] E. Gabrielli *et al.*, Nucl.Phys. **B** 362 (1991) 475.
- [3] G.P. Lepage and P.B. Mackenzie, Phys.Rev. **D** 48 (1993), 2250.
- [4] S. Naik, Phys.Lett. **B** 311, (1993), 230.
- [5] C.R. Allton *et al.*, UKQCD collaboration, Phys.Rev. **D** 47 (1993), 5128.
- [6] P. Lacock *et al.*, UKQCD collaboration, Phys.Rev. **D** 51 (1995), 6403.
- [7] C.R. Allton *et al.*, UKQCD collaboration, Phys.Rev. **D** 49 (1994), 474.
- [8] C. Michael and A. McKerrell, Phys.Rev. **D** 51 (1995), 3745.
- [9] P. Lacock and C. Michael, UKQCD Collaboration, hep-lat/9506009, University of Liverpool preprint LTH-349, Phys.Rev.D (in press).
- [10] N. Stella and C. T. Sachrajda, Private Communication.
- [11] G. Martinelli *et al.* Phys. Lett. **B** 311 (1993) 241.
- [12] C.Pittori *et al.*, Nucl.Phys. **B** (Proc.Suppl.) 42, (1995), 428.

TABLES

β	$N_s^3 \times N_t$	Number of configurations	κ	Smearing	Clover coefficient
5.7	$12^3 \times 24$	480	0.13843, 0.14077	Jacobi & Local	1.5678
6.0	$16^3 \times 48$	130	0.1370, 0.1381	Fuzzed & Local	1.4785
6.2	$24^3 \times 48$	184	0.1364, 0.1371	Local	1.4424

TABLE I. Input parameters for simulation.

β	$\tilde{\kappa}_{\text{crit}}$	$\tilde{\kappa}_{\text{crit}}^{\text{1Loop}}$	$am_\rho(\kappa_{\text{crit}})$	$a_{m\rho}^{-1}$ [GeV]
5.7	0.12344^{+2}_{-2}	0.1214	0.678^{+7}_{-7}	1.14^{+1}_{-1}
6.0	0.12218^{+3}_{-2}	0.1219	0.405^{+13}_{-12}	1.90^{+6}_{-6}
6.2	0.12206^{+1}_{-2}	0.1221	0.302^{+12}_{-14}	2.55^{+12}_{-10}

 TABLE II. Output results of simulation. Non-perturbatively derived values of $\tilde{\kappa}_{\text{crit}}$ compared with a 1-loop calculation using tadpole-improved perturbation theory. The vector masses extrapolated to the chiral limit ($m_\pi = 0$) and the resulting scale, taking $m_\rho = 0.7699$ GeV.

FIGURES

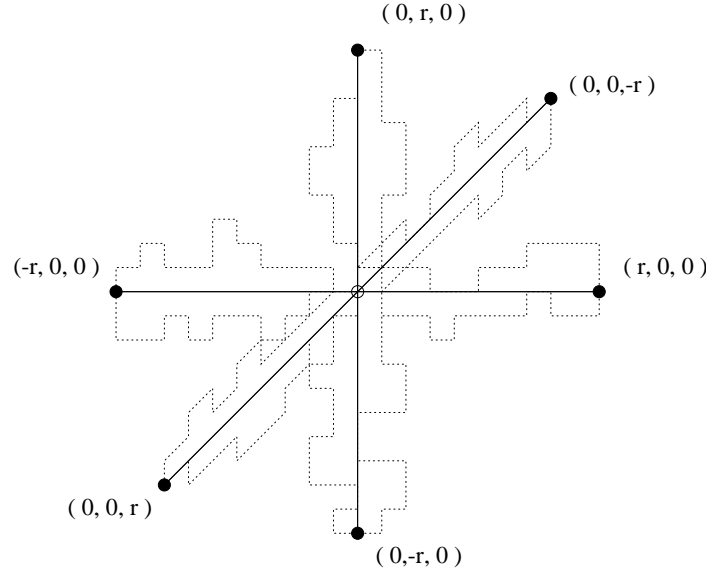


FIG. 1. Schematic guide to fuzzing. The source is composed of six points around the origin.

The dotted lines indicate typical paths that will be used in the average.

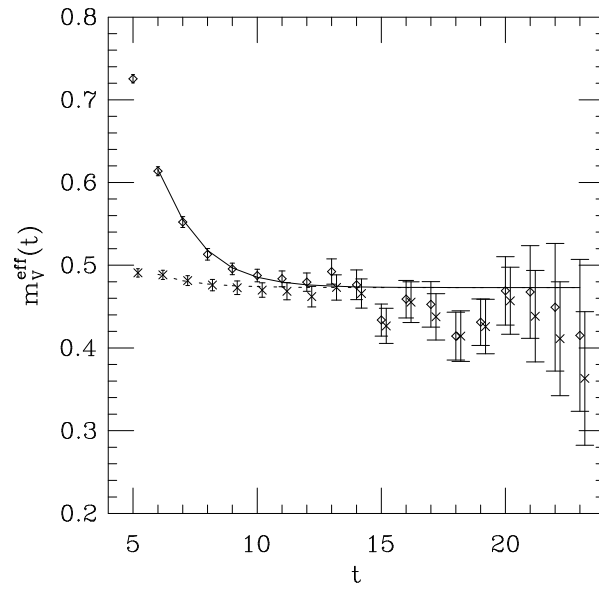


FIG. 2. The effective mass of the vector meson versus time separation t . The data are at $\beta = 6.0$ and $\kappa = 0.1381$, using local (diamonds) and fuzed (crosses) sources. The fits shown are two state expressions.

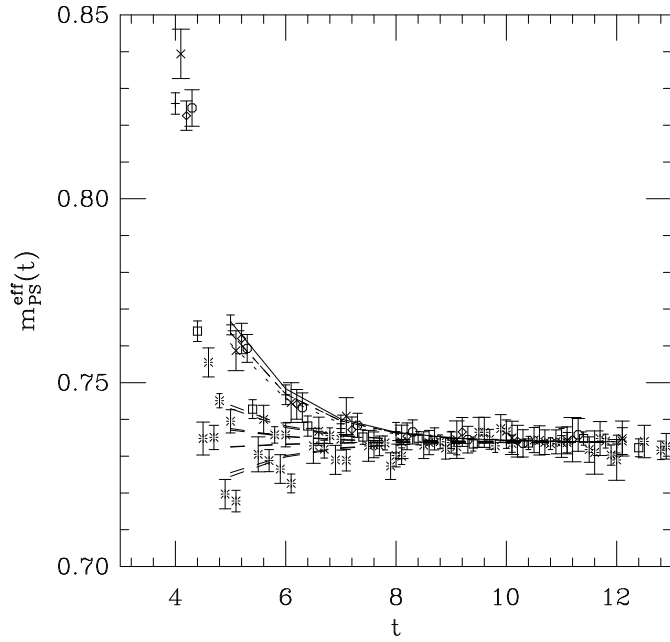


FIG. 3. Effective mass plot from the local and smeared combinations of the operators A and P at $\beta = 5.7$ and $\kappa = 0.13843$.

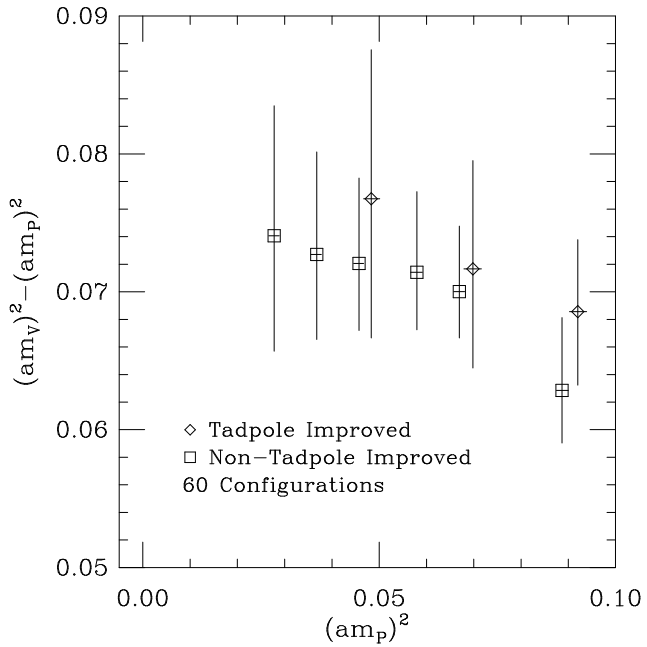


FIG. 4. The comparison of the mass combination $(am_V)^2 - (am_P)^2$ at $\beta = 6.2$ from SW-clover and tadpole-improved SW-clover fermionic actions.

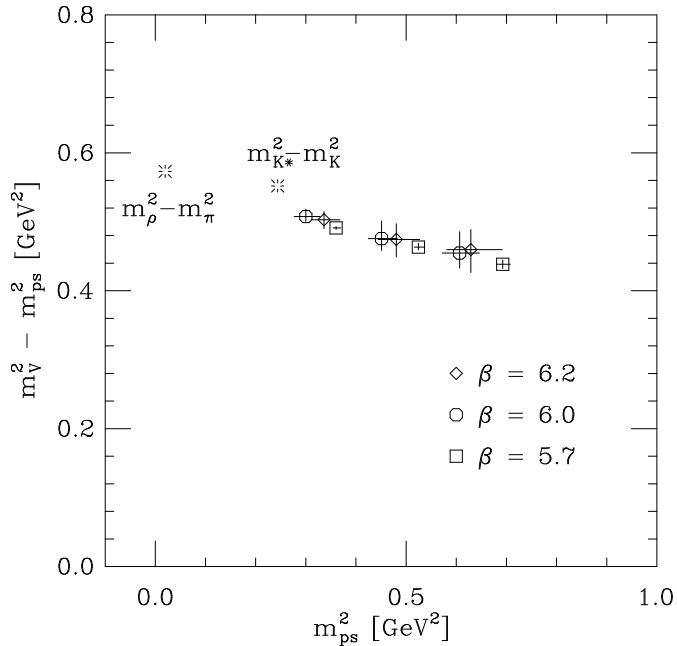


FIG. 5. The comparison of the mass combination $(m_V)^2 - (m_P)^2$ between lattice results and experiment.

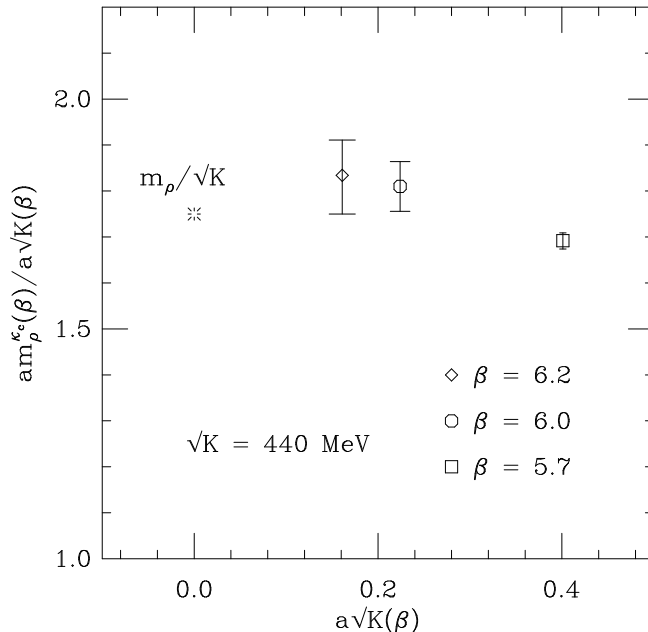


FIG. 6. The dimensionless ratio of the ρ -mass to the square root of the string tension. The “experimental” point at $a = 0$ corresponds to $(770\text{MeV}/440\text{MeV})$.

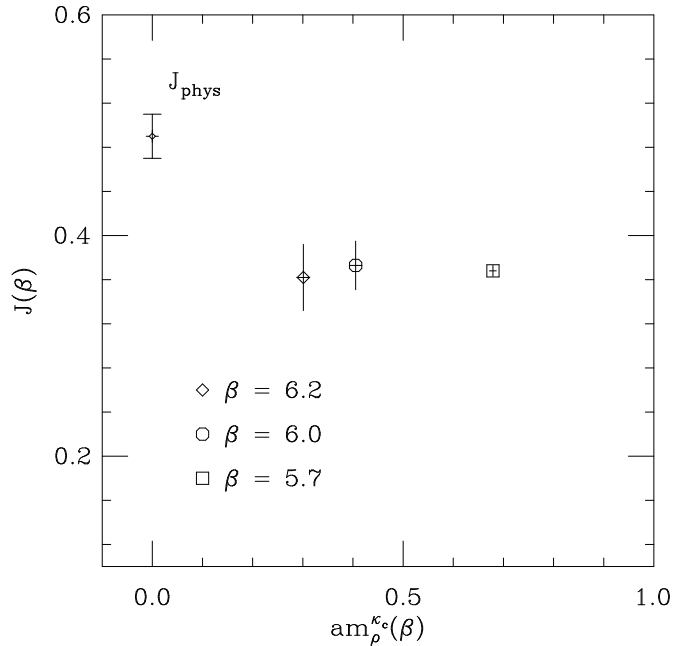


FIG. 7. The dimensionless quantity $J = m_v dm_V/dm_{PS}^2$ from the different lattice β -values compared to the experimental value.

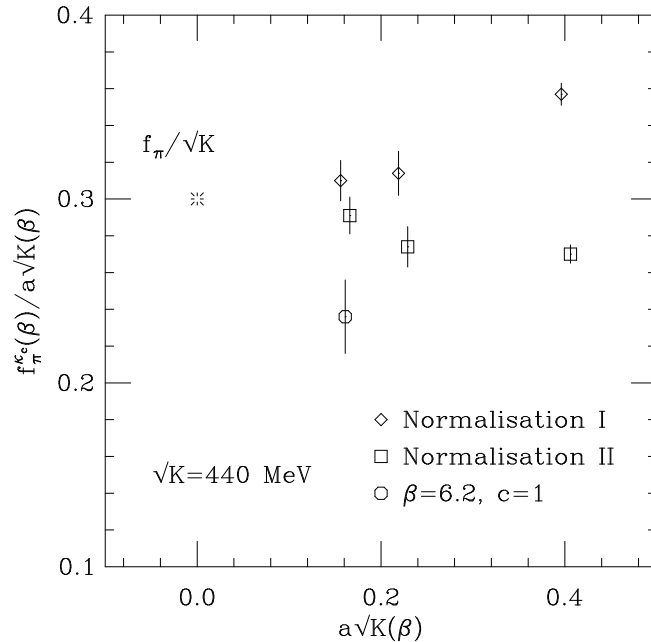


FIG. 8. The dimensionless ratio of f_π to the square root of the string tension. The “experimental” point at $a = 0$ corresponds to (132MeV/440MeV). The points are displaced slightly for clarity.

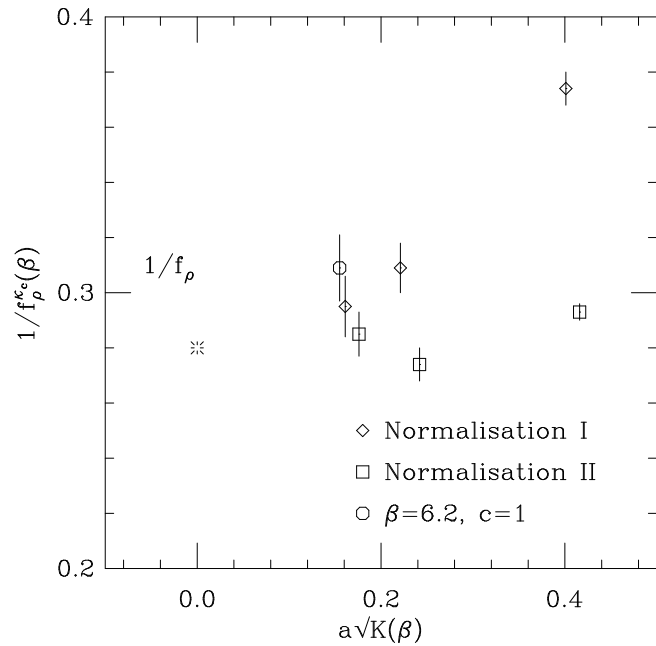


FIG. 9. The ρ meson decay constant $1/f_\rho$ versus the lattice spacing a . The points are displaced slightly for clarity.